e-ISSN 2083–4640
ISSN 1507–1367

RESEARCH PAPER

Reports of Practical Oncology and Radiotherapy
2023, Volume 28, Number 4, pages: 514–521
DOI: 10.5603/RPOR.a2023.0062
Submitted: 17.01.2023
Accepted: 03.08.2023

Biological dosimetric impact of dose-delivery time for hypoxic tumour with modified microdosimetric kinetic model

Daisuke Kawahara, Yasushi Nagata

Department of Radiation Oncology, Institute of Biomedical & Health Science, Hiroshima University, Japan

ABSTRACT

Background: An improved microdosimetric kinetic model (MKM) can address radiobiological effects with prolonged delivery times. However, these do not consider the effects of oxygen. The current study aimed to evaluate the biological dosimetric effects associated with the dose delivery time in hypoxic tumours with improved MKM for photon radiation therapy.

Materials and methods: Cell survival was measured under anoxic, hypoxic, and oxic conditions using the Monte Carlo code PHITS. The effect of the dose rate of 0.5–24 Gy/min for the biological dose (D_{bio}) was estimated using the microdosimetric kinetic model. The dose per fraction and pressure of O_2 (pO_2) in the tumour varied from 2 to 20 Gy and from 0.01 to 5.0% pO_2, respectively.

Results: The ratio of the D_{bio} at 1.0–24 Gy/min to that at 0.5 Gy/min (R_{DR}) was higher at higher doses. The maximum R_{DR} was 1.09 at 1.0 Gy/min, 1.12 at 12 Gy/min, and 1.13 at 24 Gy/min. The ratio of the D_{bio} at 0.01–2.0% of pO_2 to that at 5.0% of pO_2 (R_{oxy}) was within 0.1 for 2–20 Gy of physical dose. The maximum R_{oxy} was 0.42 at 0.01% pO_2, 0.76 at 0.4% pO_2, 0.89 at 1% pO_2, and 0.96 at 2% pO_2.

Conclusion: Our proposed model can estimate the cell killing and biological dose under hypoxia in a clinical and realistic patient. A shorter dose-delivery time with a higher oxygen distribution increased the radiobiological effect. It was more effective at higher doses per fraction than at lower doses.

Key words: microdosimetric kinetic model; dose delivery; hypoxic

Rep Pract Oncol Radiother 2023;28(4):514–521

Introduction

Treatment techniques and dose delivery have improved in radiotherapy. Intensity-modulated radiotherapy (IMRT) employs variable intensities across multiple beams. This yields highly conformal dose distributions.

IMRT generally requires multiple beams, which increases the treatment delivery time [1, 2]. Recently, volumetric modulated arc therapy (VMAT) has enabled treatment using one or two arcs [3]. The dose delivery time can be reduced compared with the IMRT technique. Stereotactic radiosurgery (SRS) and stereotactic body radiotherapy (SBRT) involve a large dose per fraction. This requires a longer dose delivery time than that for conventional radiotherapy. Recently, SBRT was combined with a flattening filter-free (FFF) beam, which uses a non-uniform beam and can reduce the treatment delivery time [4, 5].

Dose-calculation algorithms have advanced with the development of computer science. First, a fac-

Address for correspondence: Daisuke Kawahara, Department of Radiation Oncology, Institute of Biomedical & Health Science, Hiroshima University, Japan; e-mail: daika99@hiroshima-u.ac.jp

tor-based algorithm was developed that resolves surface curvature and tissue heterogeneity based on effective spatial dose measures such as the path lengths in water, field boundaries, and depth [7]. Subsequently, a model-based algorithm that predicts patient dose distributions from a dose kernel and primary particle fluence was developed [8–10]. Recently, the Monte Carlo algorithm was introduced in clinical settings. The Monte Carlo algorithm addresses the stochasticity of radiation interaction with matter [11–14]. Furuta et al. developed novel medical applications for the particle and heavy-ion transport code system (PHITS) MC package [15]. PHITS can calculate the linear energy distribution to estimate the biological effectiveness. Earlier, we investigated the biological effectiveness of Lipiodol using flattening filter (FF) and FFF beams [16]. However, the biological effectiveness of the dose delivery time has not been investigated.

A prolonged delivery time affects radiobiological damage. Elkind et al. introduced sub-lethal damage repair (SLDR). Herein, cell death tends to decrease with a longer dose delivery time [6]. Nakano et al. reported a difference in dose delivery time between FFF and flattened filter (FF) beams [17]. Moreover, we proposed a dose compensation model for biological effectiveness based on the interruption time [18]. These studies simulated radiobiological effectiveness using a microkinetic model (MKM). However, these did not investigate the impact of tumour hypoxia or a prolonged delivery time. In clinical radiotherapy, the radiosensitivity of tumour cells decreases in hypoxic regions. This plays an important role in the progression of malignancy. Hall et al. reported that at < 20%, pO_2 induced redio-resistance [19]. Hypoxia is an important factor limiting tumour prognosis. Tinganelli et al. demonstrated that the cell survival curve changes with the period during which the cells are exposed to hypoxic conditions [20]. Simulation of radiobiological effects including hypoxia and prolonged delivery time could contribute to addressing this limitation.

The current study improved the microdosimetric model by considering the oxygen dose enhancement in hypoxic tumours. Moreover, it has been used to evaluate the biological dose by varying the dose-delivery time in hypoxic tumours.

Materials and methods

Physical dose and lineal energy distribution in PHITS

To calculate the biological dose, the parameters of linear energy and physical dose were obtained from the Monte Carlo calculation code Particle and Heavy Ion Transport Code System (PHITS). The TrueBeam linear accelerator (Varian Medical Systems, Palo Alto, United States) that used phase-space files provided above the secondary jaw with a 6 MV x-ray beam was modelled in PHITS [18]. The dose was calculated in a virtual water phantom (20 × 20 × 20 cm) with a grid size of 2 mm and photon history of 4.0×10^9. The cut-off energies of photon and electron were set to 0.01 MeV and 0.7 MeV, respectively. The validation results showed that the Monte Carlo calculation and the measurement in a 0.04 cm^3–volume CC04 (IBA Dosimetry, TN, United States) chamber for a 10 × 10 cm field at an SSD of 100 cm agreed within 1.0% [16]. The linear energy distribution was calculated using the T-SED function in PHITS [22].

Survival fraction in the MKM

The oxygen enhancement ratio (OER) is calculated as the dose in hypoxia divided by that in the specific oxygen concentration to achieve an equal survival level. The OER was estimated using the hypoxia reduction factor (HRF). It is the ratio of the doses for a specific iso-effect under a given oxygenation condition to that under the condition at 21% pO_2. The MKM fit of clonogenic survival at a dose corrected for oxygen distribution was applied to predict the radiobiological effects in hypoxic tumours. The equation of HRF is used in the Howard–Flanders mathematical formalism as follows [22]:

$$HRF = \frac{mK + O_2[c],}{K + O_2[c]} \quad (1)$$

where m is the maximum HRF, $O_2[c]$ is the amount of oxygen for any cell of the tumour, and K is the oxygen partial pressure at which the HRF is half the maximum value. m and K were set as 2.7 and 0.002, respectively, and were fitted to the experimental data obtained by Paul-Gilloteaux et al. [23]. To consider the oxygen effect for the response on the tumour after radiotherapy, the HRF was applied to calculate the dose (D') corrected at

0.01% pO_2 (hypoxia causing tumour death), 0.4% (radiobiological hypoxia), 1.0% pO_2 (pathological hypoxia), 2.0% pO_2 (physiological hypoxia), and 5.0% pO_2 (physoxia) [24].

$$D' = \frac{D}{HRF} \quad (2)$$

where D denotes the physical dose. The survival fraction was calculated using the MKM method proposed by Hawkins et al [25]. The surviving fraction of cells after irradiation, as proposed in a previous study, is expressed as follows [18]:

$$-lnS = \left(\alpha_0 + \frac{y_D}{\rho\pi r_d^2}\beta_0\right)D + \beta' D^2 \quad (3)$$

where α_0 and β_0 are the proportional factors to D [Gy^{-1}] and D^2 [Gy^{-2}], respectively. The dose-mean lineal energy, y_D, was set as 2.32 keV/μm [18]. The radius of the domain, r_d, was 0.23 μm, and the density of the domain, ρ, was set as 1.0 g/cm^3. was derived from a past study [26]:

$$\beta' = \frac{2\beta_0}{(a+c)^2T^2}\left[(a+c)T\frac{\left(1+e^{-2(a+c)t_r}\right)}{\left(1-e^{-2(a+c)t_r}\right)} - 1 + \frac{e^{-(a+c)T}\left(1-e^{-2(a+c)(t_r-T)}\right)}{\left(1-e^{-2(a+c)t_r}\right)}\right] \quad (4)$$

where DR is the dose rate and T is the delivery time during irradiation. This is calculated as follows:

$$T = \frac{D}{DR} \quad (5)$$

(a + c) is defined as the potentially lethal lesion repair rate obtained from Matsuya et al. [27]. Eq. (3) can be converted using by considering the following hypoxic reduction factor:

$$-lnS = \left(\alpha_0 + \frac{y_D}{\rho\pi r_d^2}\beta_0\right)D' + \beta' D'^2 \quad (6)$$

The biological dose (D_{bio}) proposed by Inaniwa et al. [26] using Eq. 4 was computed as

$$D_{bio} = \left[-\frac{\alpha_0}{2\beta} + \sqrt{\left(\frac{\alpha_0}{2\beta}\right)^2 - \frac{lnS}{\beta}}\right] \quad (7)$$

α_0 and β_0 were estimated from the experiment survival data of CHO-K1 cells after irradiation with X-rays under various oxygen conditions of 0%, 0.5%, and 21% pO_2 [28, 29]. The CHO-K1 cells were cultured in Ham's F12 medium supplemented with 1% penicillin/streptomycin (Biochrom AG, Berlin, Germany) and 10% foetal calf serum (FCS). Cells were maintained in a humidified atmosphere containing 5% CO2 at 37°C. These cells were subcultured at a density of 5×10^4 cells in 25 cm^2 culture flasks with a 5 ml culture medium two times a week.

Biological dosimetric impact of dose-delivery time for hypoxic tumour

This study evaluated the biological dosimetric impact of the dose-delivery time on hypoxia using the following two metrics: The ratio of the biological dose with 1–24 Gy/min to that with 0.5 Gy/min for a D of 0–20 Gy at 0.01–5.0% pO_2 was defined as R_{DR}. The ratio of the biological dose at 0.01–2.0% pO_2 to that at 5.0% pO_2 was defined as R_{oxy}.

Results

Validation of the MKM in survival fraction with a different oxygen distribution

The model parameters of α_0 and β_0 were determined by fitting the model to the experiment survival data [28, 29]. Figure 1 shows the fitting curve of the simulated and experimental survival data for the oxygen concentrations of 0%, 0.5%, and 20% pO_2. The error bars indicate the standard deviations of the experimental survival data. The fit was in good agreement with the standard deviation of the experimental survival data. The fitted parameters of α_0 and β_0 were 0.22 Gy^{-1} and 0.195 Gy^{-2}, respectively.

Biological dose difference with different oxygen concentrations

Figure 2 shows the D_{bio} for the physical dose owing to the dose rate of 0.5–24 Gy/min at 0.01–5.0% pO_2. D_{bio} increased with an increase in the physical dose. The difference in D_{bio} of the dose rate was larger with a higher physical dose.

Figure 3 illustrates R_{DR}. It is defined as the ratio of the D_{bio} at 1–24 Gy/min to that at 0.5 Gy/min. R_{DR} was investigated at 0.01–5.0% pO_2. It increased with a higher physical dose. The maximum R_{DR} was 1.09 at 1 Gy/min, 1.12 at 12 Gy/min, and 1.13 at 24 Gy/min, respectively. Although the high dose rate X-ray beam had a larger R_{DR} for each physical dose, the difference in R_{DR} at 12 Gy/min and 24 Gy/min was within 1% pO_2.

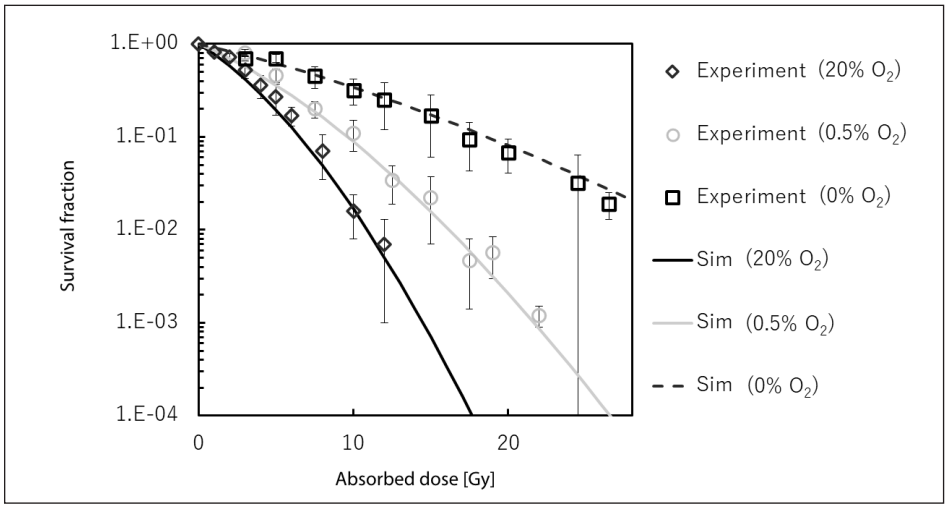

Figure 1. Survival fraction in the experiment data and the calculation data with particle and heavy-ion transport code system (PHITS)

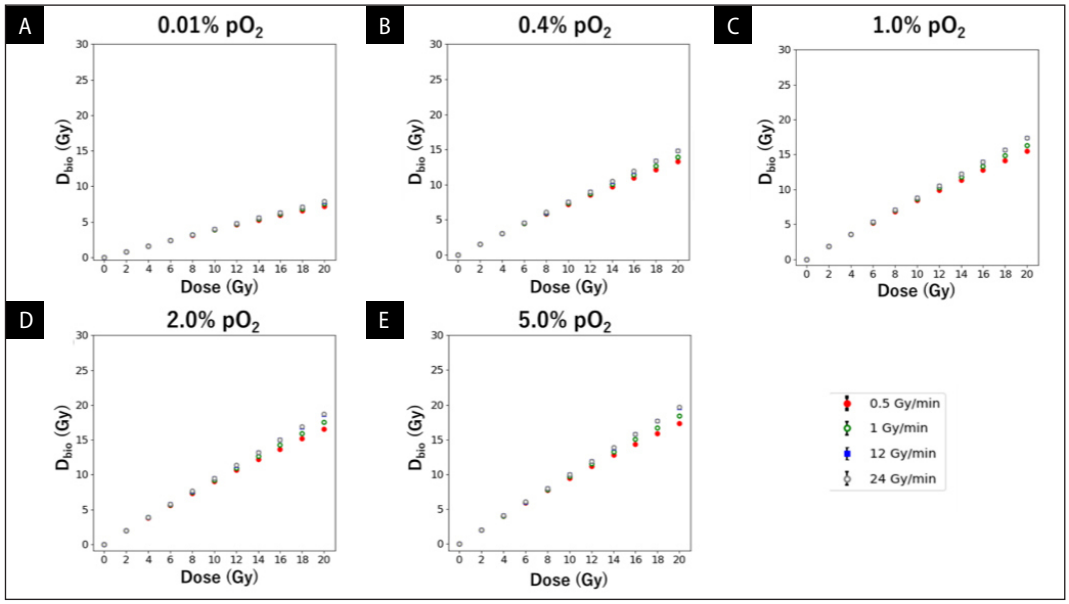

Figure 2. Biological dose for the physical dose of 2–20 Gy owing to the dose rate of 0.5–24 Gy/min at (**A**) 0.01% pressure of O_2 (pO_2), (**B**) 0.4% pO_2, (**C**) 1.0% pO_2, (**D**) 2.0% pO_2, and (**E**) 5.0% pO_2

Biological dose difference with a different dose rate

Figure 4 shows the D_{bio} for the physical dose at 0.01–5.0% pO_2 with a dose rate of 0.5–24 Gy/min. D_{bio} increased with higher concentrations of oxygen.

Figure 5 shows the R_{Oxy} at 0.01–5.0% pO_2 for a D of 0–20 Gy with a dose rate of 0.5–24 Gy/min. A higher concentration of oxygen resulted in a higher R_{Oxy}. The R_{Oxy} for a physical dose of 2–20 Gy was 0.4–0.42, 0.75–0.76, 0.88–0.89, and 0.95–0.96 at 0.01%, 0.4%, 1.0%, and 2.0% pO_2 of oxygen concentration, respectively. The difference in R_{Oxy} in the range of 2–20 Gy was within 1.0% for all the oxygen concentrations. The difference in R_{Oxy} for 0.5–24 Gy/min was also within 1.0%.

Discussion

The dose delivery time depends on the dose rate. That is, a higher dose rate can reduce the dose delivery time. This study demonstrated that a higher

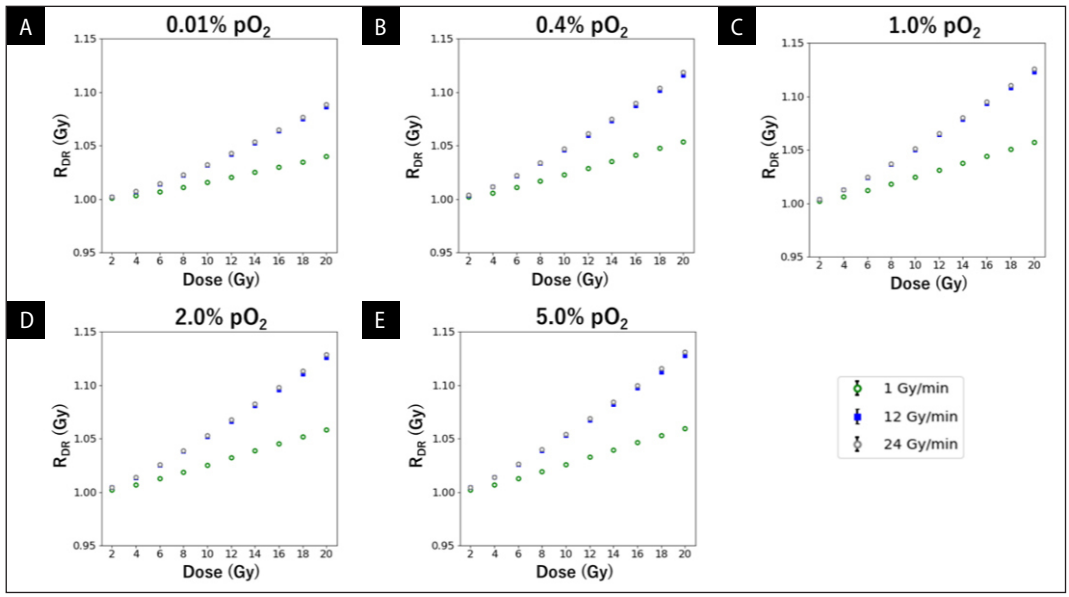

Figure 3. Ratio of the biological dose with 1–24 Gy/min to that with 0.5 Gy/min (R_{DR}) for D of 2–20 Gy at (**A**) 0.01% pressure of O_2 (pO_2), (**B**) 0.4% pO_2, (**C**) 1.0% pO_2, (**D**) 2.0% pO_2, and (**E**) 5.0% pO_2

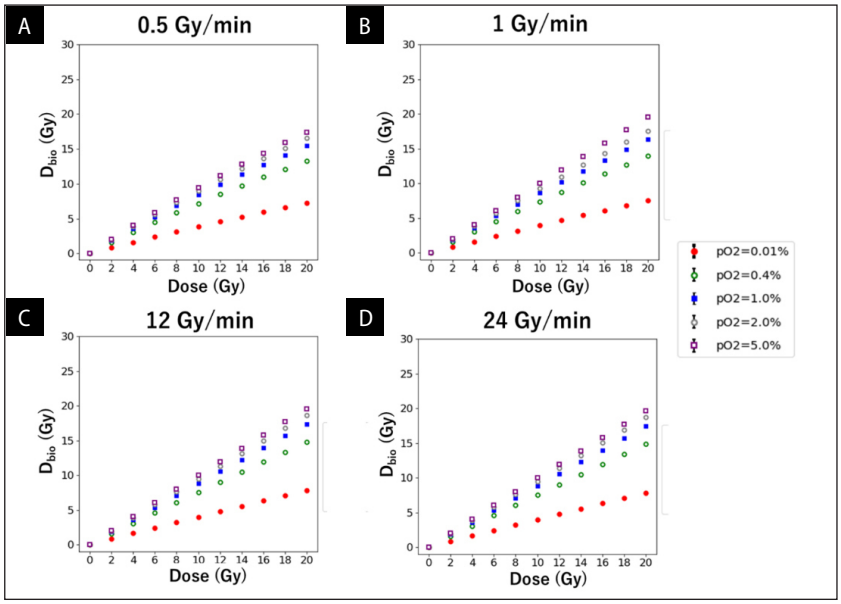

Figure 4. Biological dose *vs*. physical dose of 2–20 Gy at 0.01–5.0% pressure of O_2 (pO_2) with dose rates of (**A**) 0.5 Gy/min, (**B**) 1 Gy/min, (**C**) 12 Gy/min, and (**D**) 24 Gy/min

dose rate increased the biological dose. Brehwens et al. reported that DNA repair occurred under irradiation with a photon beam of less than 1 Gy/min [30]. In particular, FFF beams at > 12 Gy/min exhibited a larger biological effect. Nakano et al. reported that a short dose-delivery time increased the relative biological effectiveness [17]. A higher dose rate reduces the SLDR. This may cause an increase in the treatment outcome [31]. Recently, FLASH irradiation with an ultrahigh dose-rate of irradiation (> 40 Gy/s) was developed. It enables the sparing of normal tissue while retaining tumour control. Further studies would be performed to investigate the dose-rate effect in normal tissues [31].

This study investigated the effects of oxygen and the dose rates on tumours with an improved

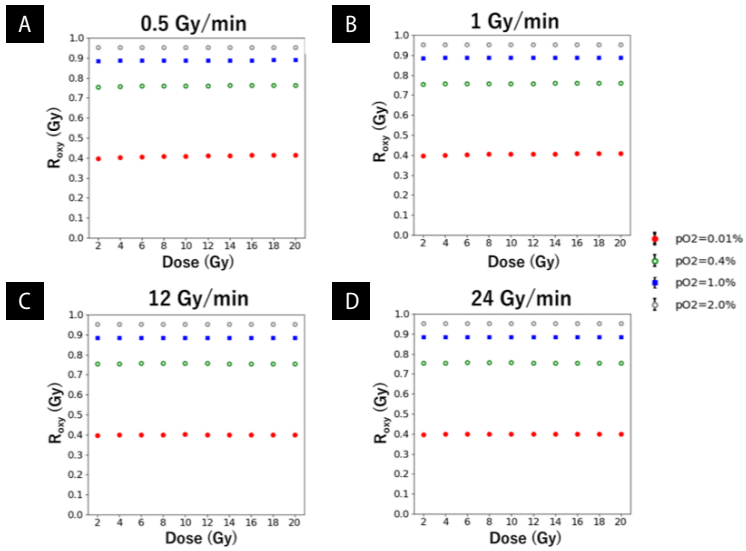

Figure 5. Ratio of the biological dose at 0.01–2.0% pO_2 to that at 5.0% pressure of O_2 (pO_2) with dose rates of (**A**) 0.5 Gy/min, (**B**) 1 Gy/min, (**C**) 12 Gy/min, and (**D**) 24 Gy/min

MKM. The biological effectiveness increased with a high concentration of oxygen and higher photon-beam dose rate. Hara et al. investigated the radiobiological effects on hypoxic and oxic cells using high- and low-dose-rate beams [32]. They showed that a higher dose rate decreased the surviving fraction. Additionally, the surviving fraction of oxic cells was lower than that of hypoxic cells at an equal photon beam dose rate. These results support the results of the simulations. The neutralisation of radiotherapy-induced reactive oxygen species decreases at higher oxygen concentrations because oxygen helps neutralise hydrated electrons. This causes an increase in the DNA damage [33, 34]. The current study showed that a beam with a higher dose rate, such as an FFF beam, shortens the dose delivery time and increases the biological effectiveness. In particular, it increased exponentially with a higher dose rate and physical dose. Moreover, the oxygen concentration helped increase the biological effectiveness, although the difference in biological effectiveness between the physical doses at each oxygen concentration was marginal.

A limitation of the current study is that other biological effects such as angiogenesis and the cell cycle were not incorporated. Our simulation incorporated a Monte Carlo calculation that can provide an accurate dose and better estimates of the biological dose or tumour control ratio for radiotherapy treatment planning and trial design by incorporating accurate radiobiological models.

Conclusions

Our proposed model could estimate the cell killing and biological dose under hypoxia in a clinical and realistic patient. A shorter dose-delivery time with a higher oxygen distribution increased the radiobiological effect. It was more effective at higher doses per fraction than at lower doses.

Conflict of interest

None declared.

Funding

None declared.

References

1. Staffurth J. Radiotherapy Development Board. A review of the clinical evidence for intensity-modulated radiotherapy. Clin Oncol (R Coll Radiol). 2010; 22(8): 643–657, doi: 10.1016/j.clon.2010.06.013, indexed in Pubmed: 20673708.
2. Veldeman L, Madani I, Hulstaert F, et al. Evidence behind use of intensity-modulated radiotherapy: a systematic review of comparative clinical studies. Lancet Oncol. 2008; 9(4): 367–375, doi: 10.1016/S1470-2045(08)70098-6, indexed in Pubmed: 18374290.
3. Otto K. Volumetric modulated arc therapy: IMRT in a single gantry arc. Med Phys. 2008; 35(1): 310–317, doi: 10.1118/1.2818738, indexed in Pubmed: 18293586.

4. Verbakel WF, van den Berg J, Slotman BJ, et al. Comparable cell survival between high dose rate flattening filter free and conventional dose rate irradiation. Acta Oncol. 2013; 52(3): 652–657, doi: 10.3109/0284186X.2012.737021, indexed in Pubmed: 23126524.
5. Lohse I, Lang S, Hrbacek J, et al. Effect of high dose per pulse flattening filter-free beams on cancer cell survival. Radiother Oncol. 2011; 101(1): 226–232, doi: 10.1016/j.radonc.2011.05.072, indexed in Pubmed: 21733592.
6. Elkind MM, Sutton H. Radiation response of mammalian cells grown in culture. 1. Repair of X-ray damage in surviving Chinese hamster cells. Radiat Res. 1960; 13: 556–593, indexed in Pubmed: 13726391.
7. Khan FM, Levitt SH, Moore VC, et al. Computer and approximation methods of calculating depth dose in irregularly shaped fields. Radiology. 1973; 106(2): 433–436, doi: 10.1148/106.2.433, indexed in Pubmed: 4684488.
8. Hogstrom KR, Mills MD, Almond PR. Electron beam dose calculations. Phys Med Biol. 1981; 26(3): 445–459, doi: 10.1088/0031-9155/26/3/008, indexed in Pubmed: 6787621.
9. Scholz C, Schulze C, Oelfke U, et al. Development and clinical application of a fast superposition algorithm in radiation therapy. Radiother Oncol. 2003; 69(1): 79–90, doi: 10.1016/s0167-8140(03)00205-6, indexed in Pubmed: 14597360.
10. Ahnesjö A. Collapsed cone convolution of radiant energy for photon dose calculation in heterogeneous media. Med Phys. 1989; 16(4): 577–592, doi: 10.1118/1.596360, indexed in Pubmed: 2770632.
11. Kurosu K, Das I, Moskvin V. Optimization of GATE and PHITS Monte Carlo code parameters for spot scanning proton beam based on simulation with FLUKA general-purpose code. Nucl Instrum Methods Phys Res, Sect B. 2016; 367: 14–25, doi: 10.1016/j.nimb.2015.11.017.
12. Shahmohammadi Beni M, Krstic D, Nikezic D, et al. A comparative study on dispersed doses during photon and proton radiation therapy in pediatric applications. PLoS One. 2021; 16(3): e0248300, doi: 10.1371/journal.pone.0248300, indexed in Pubmed: 33690664.
13. Shahmohammadi Beni M, Krstic D, Nikezic D, et al. A calibration method for realistic neutron dosimetry in radiobiological experiments assisted by MCNP simulation. J Radiat Res. 2016; 57(5): 492–498, doi: 10.1093/jrr/rrw063, indexed in Pubmed: 27380801.
14. Furuta T, Sato T. Medical application of particle and heavy ion transport code system PHITS. Radiol Phys Technol. 2021; 14(3): 215–225, doi: 10.1007/s12194-021-00628-0, indexed in Pubmed: 34195914.
15. Islam MdS, Watanuki S, Tashiro M, et al. Internal radiation dose estimation using multiple D-shuttle dosimeters for positron emission tomography (PET): A validation study using NEMA body phantom. Med Phys. 2018; 45(10): 4693–4703, doi: 10.1002/mp.13124, indexed in Pubmed: 30098031.
16. Kawahara D, Nakano H, Ozawa S, et al. Relative biological effectiveness study of Lipiodol based on microdosimetric-kinetic model. Phys Med. 2018; 46: 89–95, doi: 10.1016/j.ejmp.2018.01.018, indexed in Pubmed: 29519415.
17. Nakano H, Kawahara D, Ono K, et al. Effect of dose-delivery time for flattened and flattening filter-free photon beams based on microdosimetric kinetic model. PLoS One. 2018; 13(11): e0206673, doi: 10.1371/journal.pone.0206673, indexed in Pubmed: 30462672.
18. Kawahara D, Nakano H, Saito A, et al. Dose compensation based on biological effectiveness due to interruption time for photon radiation therapy. Br J Radiol. 2020; 93(1111): 20200125, doi: 10.1259/bjr.20200125, indexed in Pubmed: 32356450.
19. Hall EJ, Giaccia AJ. Oxygen Effect and Reoxygenation. In: Hall EJ, Giaccia AJ. ed. Radiobiology for the Radiologist. 7th ed. Lippincott Williams & Wilkins, Philadelphia 2010: 96–103.
20. Tinganelli W, Ma NY, Von Neubeck C, et al. Influence of acute hypoxia and radiation quality on cell survival. J Radiat Res. 2013; 54 Suppl 1(Suppl 1): i23–i30, doi: 10.1093/jrr/rrt065, indexed in Pubmed: 23824123.
21. Sato T, Watanabe R, Niita K. Development of a calculation method for estimating specific energy distribution in complex radiation fields. Radiat Prot Dosimetry. 2006; 122(1-4): 41–45, doi: 10.1093/rpd/ncl407, indexed in Pubmed: 17132656.
22. Howard-Flanders P, Alper T. The sensitivity of microorganisms to irradiation under controlled gas conditions. Radiat Res. 1957; 7(5): 518–540, indexed in Pubmed: 13485393.
23. Paul-Gilloteaux P, Potiron V, Delpon G, et al. Optimizing radiotherapy protocols using computer automata to model tumour cell death as a function of oxygen diffusion processes. Sci Rep. 2017; 7(1): 2280, doi: 10.1038/s41598-017-01757-6, indexed in Pubmed: 28536438.
24. McKeown SR. Defining normoxia, physoxia and hypoxia in tumours-implications for treatment response. Br J Radiol. 2014; 87(1035): 20130676, doi: 10.1259/bjr.20130676, indexed in Pubmed: 24588669.
25. Hawkins RB. A microdosimetric-kinetic model of cell death from exposure to ionizing radiation of any LET, with experimental and clinical applications. Int J Radiat Biol. 1996; 69(6): 739–755, doi: 10.1080/095530096145481, indexed in Pubmed: 8691026.
26. Inaniwa T, Kanematsu N, Suzuki M, et al. Effects of beam interruption time on tumor control probability in single-fractionated carbon-ion radiotherapy for non-small cell lung cancer. Phys Med Biol. 2015; 60(10): 4105–4121, doi: 10.1088/0031-9155/60/10/4105, indexed in Pubmed: 25933161.
27. Matsuya Y, McMahon SJ, Ghita M, et al. Intensity Modulated Radiation Fields Induce Protective Effects and Reduce Importance of Dose-Rate Effects. Sci Rep. 2019; 9(1): 9483, doi: 10.1038/s41598-019-45960-z, indexed in Pubmed: 31263149.
28. Ma NY, Tinganelli W, Maier A, et al. Influence of chronic hypoxia and radiation quality on cell survival. J Radiat Res. 2013; 54 Suppl 1(Suppl 1): i13–i22, doi: 10.1093/jrr/rrs135, indexed in Pubmed: 23824117.
29. Tinganelli W, Ma NY, Von Neubeck C, et al. Influence of acute hypoxia and radiation quality on cell survival. J Radiat Res. 2013; 54 Suppl 1(Suppl 1): i23–i30, doi: 10.1093/jrr/rrt065, indexed in Pubmed: 23824123.
30. Brehwens K, Staaf E, Haghdoost S, et al. Cytogenetic damage in cells exposed to ionizing radiation under conditions of a changing dose rate. Radiat Res. 2010; 173(3): 283–289, doi: 10.1667/RR2012.1, indexed in Pubmed: 20199213.
31. Velalopoulou A, Karagounis IV, Cramer GM, et al. FLASH Proton Radiotherapy Spares Normal Epithelial

and Mesenchymal Tissues While Preserving Sarcoma Response. Cancer Res. 2021; 81(18): 4808–4821, doi: 10.1158/0008-5472.CAN-21-1500, indexed in Pubmed: 34321243.
32. Hara T, Tominaga M, Yajyu K, et al. Effect of dose rate on antitumor activity in hypoxic cells by using flattening filter free beams. Int J Radiat Res. 2018; 16(2): 197–205.
33. Bristow RG, Hill RP. Hypoxia and metabolism. Hypoxia, DNA repair and genetic instability. Nat Rev Cancer. 2008; 8(3): 180–192, doi: 10.1038/nrc2344, indexed in Pubmed: 18273037.
34. Hirayama R. [Mechanism of oxygen effect for photon and heavy-ion beams]. Igaku Butsuri. 2014; 34(2): 65–69, indexed in Pubmed: 25693293.